

Graphene nanoribbon array in a cellular automata architecture for propagation of binary information

A. León,^{1,a)} Z. Barticevic,² and M. Pacheco^{2,a)}

¹Facultad de Ingeniería, Universidad Diego Portales, Ejército 441 Santiago, Chile

²Departamento de Física, Universidad Técnica F. Santa María, Casilla 110 V, Valparaíso, Chile

(Received 16 January 2009; accepted 8 April 2009; published online 29 April 2009)

In this work we propose a cellular automata architecture using graphene nanoribbon arrays with spin polarization. We study the electronic and magnetic properties of the proposed structures by using first principles calculations and an algorithm based in the Glauber dynamic for simulating the cellular automata evolution. Our results show that the studied system can be scaled so that the propagation of digital information throughout the automata is possible at room temperature. © 2009 American Institute of Physics. [DOI: 10.1063/1.3127231]

The limit of miniaturization of the electronic devices is reached for sizes where the system dynamic is governed by the quantum mechanics. Because of that, great efforts have been done in looking for different technologies for processing and storing information that can efficiently replace the classic electronics. One of the attempts for getting more advanced information processors has been the postulation of quantum systems to realize computation.¹ The great advantage of the physical implementation of quantum computing is the possibility of solving multiple numerical problems which cannot be solved with classical digital computers. However, for large scale systems the problem of decoherence has not been solved yet. Some significative experimental advances have been reported to face this problem by using delocalized qubits and global control protocols² in small molecular systems.

A completely different solution to the problem of the physical implementation of logic computation is the concept of the Quantum Cellular Automata, which allows to develop classical computation processes with quantum entities. Important advances have been achieved by using cellular automata composed by quantum dot arrays (QDCA), the original idea was proposed by Lent *et al.*,³ and it consists of a set of quantum corrals containing four quantum dots, doped with two electrons. These extra electrons can quantum-mechanically tunnel between dots but, cannot tunnel between the cells forming the automaton. This QDCA architecture is able to propagate and to process binary information by means of adequate control protocols.⁴ The experimental demonstration of a implementation of a QDCA was published in 1997 by Orlov *et al.*⁵ Posteriorly, the experimental implementation of a logic gate and a shift register were also reported^{6,7} with good agreement between the theoretical predictions and low temperature experimental data.

A room-temperature implementation of a QDCA requires cells with molecular size. In this context, some important experimental contributions have been reported,⁸ but more development of the device fabrication technology is still missing. Another room-temperature QDCA implementation is a magnetic quantum dot array which can propagate magnetic excitations for processing digital information.⁹ In these systems, the magnetic dipolar interaction between sub-

micrometer particles is used to perform logic operations and propagate information. In this work we propose the implementation of a cellular automaton with cells containing graphene nanoribbons (GNRCA). This kind of carbon-based nanostructures can be obtained by different experimental techniques.^{10–13}

In our study we will consider our GNRCA with cells composing by finite GNRs passivated with hydrogen molecules, these structures are also known as polycyclic aromatic hydrocarbons. In Fig. 1 we have displayed two C₄₄H₁₈ finite GNRs. The electronic and magnetic properties of the systems are obtained by means of first principles calculations based on the pseudo-potentials method and by using the generalized gradient approximation Perdew–Burke–Ernzerhof with spin polarization.¹⁴ All structures are relaxed using the Direct Inversion Iterative Subspace method¹⁵ with a residual force criteria less than 10⁻⁴ Hartree/bohr. Calculations were performed using the OPENMX Code.¹⁶ We found that the minimum energy state of this GNR presents spin polarization along the zigzag-type edges (corresponding to the edges containing more carbon atoms).^{17–20} This state is degenerate as it is shown in Fig. 1, therefore we can define the 0 or 1 logical states for the automata.

By considering a cluster formed by two interacting finite ribbons we found the distance for which the total energy of the cluster is minimum. This energy minimum occurs when the nearer edges of the ribbons have opposite total density spin polarization, i.e., energy states with configurations 00 or 11, we call it the “antiferromagnetic state” (AS). Furthermore, this system also presents a metastable state with spin

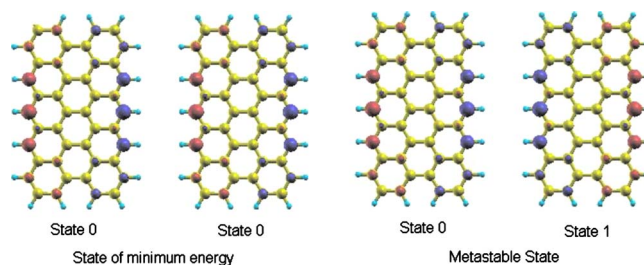


FIG. 1. (Color online) Minimum energy state (left panel) and metastable state (right panel) for a system of two C₄₄H₁₈ molecules. Black balls (red online) represent the spin up total density and gray balls (blue online) represent the spin down total density.

^{a)}Electronic addresses: alejandro.leon@udp.cl and monica.pacheco@usm.cl.

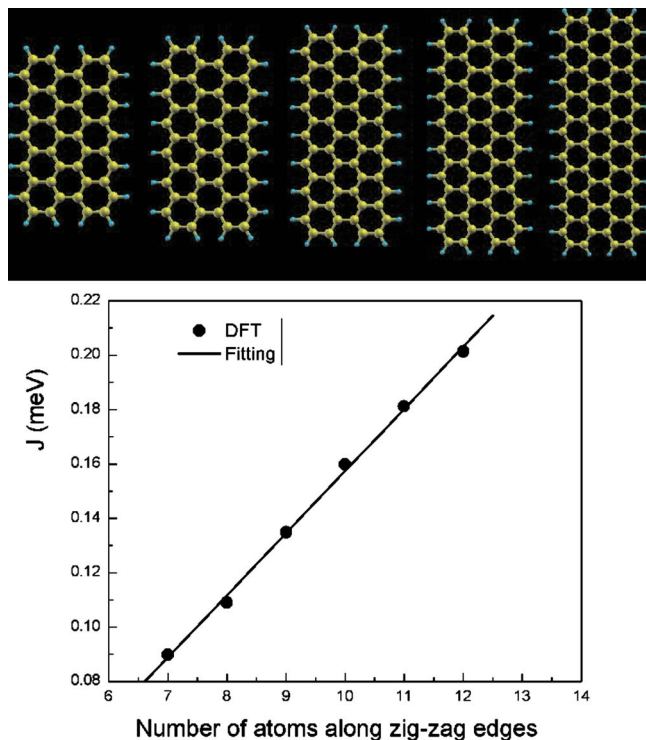


FIG. 2. (Color online) Superexchange energy parameter of in millielectron volt as a function of the number of carbon atoms along the zigzag edges.

polarizations of 01 or 10 for neighbor edges with the same type of spin polarization, we call it “ferromagnetic state” (FS). These are the two kinds of states represented in Fig. 1. For this cluster the energy separation between the states FS and AS is $\Delta E(\text{FS}-\text{AS})=0.0629$ meV. This difference in energy is very little as compared with the energy separation between the FS (or AS) state and the paramagnetic state calculated without spin polarization (corresponding to 278 meV for the molecule of $\text{C}_{44}\text{H}_{18}$).

The energy separation between the states AS and FS is usually referred in the cellular automata literature as “kink energy” E_k . In the context of magnetic properties we call it the parameter of “superexchange” between cells $J=E_k$. To postulate these systems as room-temperature binary information processors we have to study the feasibility of this superexchange effect, which we have found for small structures as not limited in scaling. We have performed the same study for longer nanoribbons with more atoms along its zigzag edges. Our results are displayed in Fig. 2 and they indicate that effectively this effect can be scaled to greater size systems. To verify that the scaling works linearly for very long ribbons we have performed first principles calculations for two infinitely long GNRs. To do this we built a tridimensional (3D) crystal but considering only interaction between the two GNRs. Figure 3 shows a scheme in the X - Y plane, in the Z direction the ribbon separation was 15 \AA . We consider three unitary cells with a different number of atoms along the zigzag edges $N_z=9, 10, 11$. Our results show that independent of the size of the unitary cell the normalized J parameter is $J(\text{meV})/N_z=0.022$ which corresponds to the slope obtained in the case of the finite nanoribbons in Fig. 2.

The dynamic response of the GNRCA is studied by implementing an “accelerated algorithm for discrete systems,”²¹ based in the Glauber dynamics.²² To perform this study we must define a unit of time for doing the simulation.

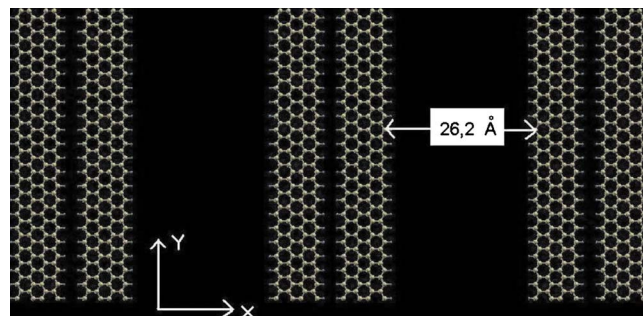


FIG. 3. (Color online) Scheme in the X - Y plane of the 3D crystal used to perform the calculation of the J value for two infinite ribbons in the Z direction the ribbon separation was 15 \AA .

Due to the phenomenon of spin polarization has a completely quantum origin, we will use the evolution propagator to estimate the time for the signal transmission. The system consisting of two finite GNRs, such as the one shown in Fig. 1, can be seen as a two-level system so a general state of the system can be written as $|\psi\rangle=ae^{-i\omega t}|0\rangle+be^{i\omega t}|1\rangle$ with $\omega=\Delta E/2\hbar$ where $\Delta E=J$. With this frequency and a threshold J value of 150 meV, we define the time unit adopted in modeling the dynamic behavior of the automaton as $T=\hbar/\pi J \approx 10^{-15}$ s.

We intend to study the form in the binary information is propagated through a molecular wire formed by N cells. To do this we must have one or more control cells that trigger the change in the state of the GNRCA. By defining n_c as the number of control cells that change simultaneously its polarization spin state under an external excitation, then the input parameters for the GNRCA dynamic simulation will be N , n_c , J , and the system temperature T .

The results indicate the existence of a threshold value for the superexchange parameter J for a given temperature, above that value the automaton state can be changed and it will remain in that state, meanwhile the control cell cannot be changed. The threshold value of J is obtained by the following procedure: (1) for an automaton of N cells (GNRs) and with n_c control cells, it is defined as an initial configuration with all cells having the same polarization state (+1 or -1). The magnetization will be given by: $M=(1/N)\sum_{j=1}^N m_j$, where m_j is the polarization of each cell. (2) For a temperature T and a given value of J , the control cell polarization is reversed and an average value for the magnetization of the whole automaton is calculated for a sufficiently long time (infinite time compared with the automaton operation time). The top panel of Fig. 4 shows the study for automata with 3, 4, 5, and 6 cells, and one control cell ($n_c=1$). All cells are in an initial configuration -1. The polarization of the first cell is changed to +1 and then it is waited for $t=30$ ps. We can see that for all values of the parameter J , the average magnetization is always positive because the polarization of the control cell remains fixed in +1, and the rest oscillates between -1 and +1. For the molecular automaton that works as a cable, it is expected that once the polarization of the control cell changes, the other cells also change and they remain in the new state of polarization (meanwhile the polarization of the cell control does not change). In the study illustrated in the Fig. 4 it is observed that for $T=300$ K the J value for which that state is reached is close to $J=150$ meV for all automata. This value increases with the

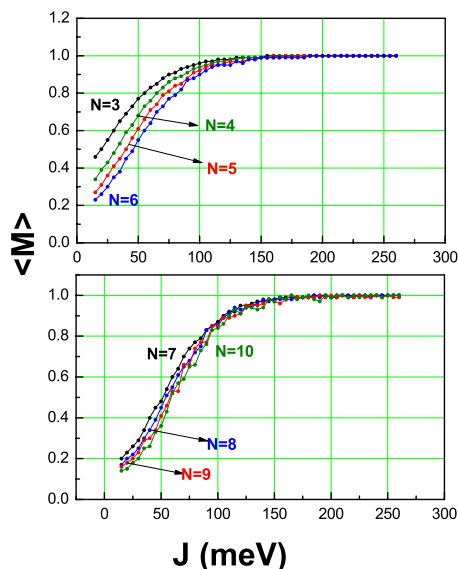


FIG. 4. (Color online) Upper panel shows the average of the magnetization as a function of J for automata with one control cell and $N=3, 4, 5,$ and 6 cells, respectively. Lower panel shows the same study for automata with $N=7, 8, 9,$ and 10 cells.

number of cells in the automaton, as shown in the bottom panel of Fig. 5 for automata with $n_c=1$ and $N=7, 8, 9,$ and 10 , respectively. To obtain this value for J the former study of scaling shows that it would be required ribbons of an approximated length of $2.1 \mu\text{m}$ along the zigzag edges.

Figure 5 shows a simulation for an automaton with a variable number of control cells. The figure displays the time (in picosecond) that the signal takes to go from one end to the other as a function of the number N of cells for $T=300 \text{ K}$, $J=150 \text{ meV}$, and n_c from 1 to 4. It can be observed that the time increases exponentially with the number of cells N and it decreases linearly with the number of control cells.

This study shows that it is possible to propagate binary information through cellular automata based on carbon-based nanostructures. We have analyzed other types of shaped graphene fragments, for instance triangular structures

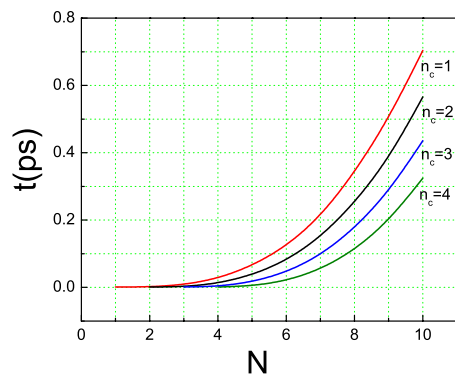


FIG. 5. (Color online) Time taken by the signal to travel from one end to the other of the automaton as a function of the total number of cells. The simulation was performed for $J=150 \text{ meV}$ and $T=300 \text{ K}$. Different curves represent simulations with distinct number of control cells.

that have the advantages of having an even number of them in the automaton, an inverter logic gate could be automatically implemented. Other structures studied are Z-shaped ribbons²³ and antidot lattices formed by holes with zigzag edges on a graphene nanoribbon.²⁴ The disadvantage of these types of clusters arises from the difficulty in the synthesis process and scaling. The systems of graphene nanoribbons proposed in this work are scalable for working at room temperature. Besides, standard lithographic techniques and other controlled cutting processes²⁵ can be used for creating graphene nanoribbons with zigzag edges and length desired. In a next article we will report the topology of the arrays for defining universal logical gates.

We acknowledge financial support of CONICYT/PBCT (CENAVA) (Grant No. ACT27), UTFSM internal grant, and Proyecto Semilla Primavera 2007-2008, UDP.

¹M. A. Nielsen and I. L. Chung, *Quantum Computation and Quantum Information* (Cambridge University Press, Cambridge, 2003).

²J. Fitzsimons, L. Xiao, S. C. Benjamin, and J. A. Jones, *Phys. Rev. Lett.* **99**, 030501 (2007).

³C. S. Lent, P. D. Tougaw, W. Porod, and G. H. Bernstein, *Nanotechnology* **4**, 49 (1993).

⁴A. I. Csurgay, W. Porod, and C. S. Lent, *IEEE Trans. Circuits Syst., I: Regul. Pap.* **47**, 1212 (2000).

⁵A. O. Orlov, I. Amlani, G. H. Bernstein, C. S. Lent, and G. L. Snider, *Science* **277**, 928 (1997).

⁶I. Amlani, A. O. Orlov, G. Toth, G. H. Bernstein, C. S. Lent, and G. L. Snider, *Science* **284**, 289 (1999).

⁷R. K. Kummamuru, A. O. Orlov, C. S. Lent, G. H. Bernstein, and G. L. Snider, *IEEE Trans. Electron Devices* **50**, 1906 (2003).

⁸J. Jiao, G. J. Long, F. Grandjean, A. M. Beatty, and T. P. Fehlner, *J. Am. Chem. Soc.* **125**, 7522 (2003).

⁹M. Macucci, *Quantum Cellular Automata* (Imperial College Press, London, 2006).

¹⁰K. S. Novoselov, A. K. Geim, S. V. Morozov, D. Jiang, Y. Zhang, S. V. Dubonos, I. V. Grigorieva, and A. A. Firsov, *Science* **306**, 666 (2004).

¹¹C. Berger, Z. Song, X. Li, X. Wu, N. Brown, C. Naud, D. Mayou, T. Li, J. Hass, A. N. Marchenkov, E. H. Conrad, P. N. First, and W. A. de Heer, *Science* **312**, 1191 (2006).

¹²M. Y. Han, B. Özyilmaz, Y. Zhang, and P. Kim, *Phys. Rev. Lett.* **98**, 206805 (2007).

¹³H. B. Heersche, P. Jarillo-Herrero, J. B. Oostinga, L. M. K. Vandersypen, and A. F. Morpurgo, *Nature (London)* **446**, 56 (2007).

¹⁴J. P. Perdew, K. Burke, and M. Ernzerhof, *Phys. Rev. Lett.* **77**, 3865 (1996).

¹⁵P. Csaszar and P. Pulay, *J. Mol. Struct.: THEOCHEM* **114**, 31 (1984).

¹⁶<http://www.openmx-square.org>

¹⁷Y. W. Son, M. L. Cohen, and S. G. Louie, *Nature (London)* **444**, 397 (2006).

¹⁸D. Jiang, B. G. Sumpter, and S. Dai, *J. Chem. Phys.* **127**, 124703 (2007).

¹⁹W. L. Wang, S. Meng, and E. Kaxiras, *Nano Lett.* **8**, 241 (2008).

²⁰J. Fernandez-Rossier and J. J. Palacios, *Phys. Rev. Lett.* **99**, 177204 (2007).

²¹W. Krauth, *Statistical Mechanics: Algorithms and Computations* (Oxford University Press, New York, 2006).

²²R. J. Glauber, *J. Math. Phys. (Cambridge, Mass.)* **4**, 294 (1963).

²³A. León, Z. Barticevic, and M. Pacheco, *Microelectron. J.* **39**, 1239 (2008).

²⁴L. Rosales, M. Pacheco, A. León, Z. Barticevic, A. Latgé, and P. Orellana, "Transport Properties of Antidot Superlattices of Graphene Nanoribbons" *Phys. Rev. B* (submitted).

²⁵L. Ci, Z. Xu, L. Wang, W. Gao, F. Ding, K. F. Kelly, B. I. Yakobson, and P. M. Ajayan, *Nano Res.* **1**, 116 (2008).